Adaptive Doppler Filtering Applied to Modern Air Traffic Control Radars

Karen J. Anderson
Dr. James Ward
Dr. Robert M. O'Donnell
MIT Lincoln Laboratory
244 Wood Street, Lexington Massachusetts 02420

Abstract - **This paper presents an analysis of the Doppler processing technology currently in use in the nation's terminal airport surveillance radars, and examines possibilities for performance improvement, particularly in the presence of moving clutter. The research focuses on five- and eight-pulse waveform methodologies and their respective detection capabilities given clearly defined rain clutter scenarios. Performance with fixed coefficient filters similar to those used in the existing radars is calculated, followed by performance using an adaptive Doppler filtering technique. Performance is quantified in terms of signal-to-interference ratio at the output of the Doppler filters and resultant probability of detection given a specified probability of false alarm. The results will show that a substantial improvement in detection in the vicinity of rain clutter is realized for both the five- and eight-pulse waveforms when using the adaptive coefficient Doppler filters as compared to the performance observed with the fixed coefficient filters. For constant filter weights, the eight-pulse Doppler filters give significantly better performance in most diverse rain clutter than the five-pulse Doppler filters.**

I. INTRODUCTION

Primary surveillance radar in air traffic control (ATC) has a renewed importance in light of recent world events. The S-band primary terminal surveillance radars, servicing the areas immediately surrounding the nation's airports, originally employed moving target indicator (MTI) detectors to cancel ground clutter. MTI radars, however, suffered detection deficiencies due to false alarms from moving clutter such as weather, birds, and ground vehicles. In the early 1970s, Lincoln Laboratory developed moving target detection (MTD) technology under Federal Aviation Administration (FAA) sponsorship for use in the airport surveillance radars (ASRs) [1]. MTD employs Doppler filter processing followed by several levels of adaptive editing to distinguish aircraft targets from stationary and moving clutter returns. The original MTD utilized two coherent processing intervals (CPIs) of ten pulses each at two different pulse repetition frequencies (PRFs). For each ten-pulse CPI, a bank of eight Doppler filters was formed to process the unambiguous Doppler interval into multiple Doppler bins. This processing technique provided a vast improvement over MTI technology, as it resulted in enhanced clutter-free detection as well as a substantial reduction in false alarm rate. As processing power improved in the late 1970s, a next-generation version of MTD evolved that incorporated better implementation of the original MTD ideas. This MTD-II system used a ten-pulse CPI followed by an eight-pulse CPI at two different PRFs, with Doppler filter banks of ten and eight filters each, respectively. The technology employed in the MTD-II system was extensively field tested and later transferred to industry for commercial production in the 1980s by Westinghouse Corporation (now Northrop Grumman). This radar, called the ASR-9, replaced the existing ASR systems at the nation's busiest airports. In the same 1980s timeframe, Raytheon Corporation developed a four-pulse, solid-state, L-band Doppler processor in Canada for the Canadian Radar Modernization Project (RAMP). Later, Raytheon applied the four-pulse Doppler filtering to an S-Band air surveillance radar. More recently, the Raytheon concept was applied to an S-band, solid-state, frequency-diverse, five-pulse Doppler processor in the ASR-11, and chosen by the FAA to replace the aging ASR-7 and -8 MTI radars that are still in use at the nation's medium-density airports.

This research focuses on the state of Doppler processing technology employed in today's ATC terminal surveillance radars and the possibilities for performance improvement, particularly in the presence of moving clutter. The study is not a direct performance comparison of the ASR-9 and ASR-11, nor does it consider other radar design parameters beyond Doppler processing that are often used to improve performance (such as frequency diversity or adaptive post-processing); rather, the investigation centers on the performance that can be expected with current Doppler techniques and then expands to consider analytically how that performance might be improved with a different Doppler filtering approach. Specifically, the paper examines both the five- and eight-pulse waveform methodologies and their respective detection capabilities given clearly defined rain clutter scenarios. Fixed coefficient Doppler filters, with amplitude and phase weights that are typical for the waveforms in question, are defined. Performance is quantified in terms of signal-to-interference ratio at the output of the Doppler filter banks and resultant probability of detection given a specified probability of false alarm. Next, an adaptive Doppler filtering technique is applied to each waveform to determine if detection improvement is possible given the

*This work is sponsored by the United States Air Force under Air Force Contract F19628-00-C-0002. Opinions, interpretations, recommendations and conclusions are those of the author and are not necessarily endorsed by the United States Government.

0-7803-8234-X/04/$17.00 © 2004 IEEE

previously defined clutter scenarios. New filter banks are generated with coefficients adapted to the clutter scenario under investigation. The results will show that a substantial improvement in detection in the vicinity of rain clutter is realized for both the five- and eight-pulse waveforms when using the adaptive coefficient Doppler filters as compared to the performance observed with the fixed coefficient filters. For constant filter weights, the eight-pulse Doppler filters give significantly better performance in most diverse rain clutter than the five-pulse Doppler filters.

II. ANALYSIS

A. Performance Measurement

For both the eight- and five-pulse waveforms, performance results are analyzed in terms of signal-to-interference ratio at the output of the Doppler filter bank and probability of detection. Output signal-to-interference ratio for the kth filter in the filter bank is defined as:

$$(SIR)_{o(k)} = S_o(f)_k / E\{\mathbf{Y}^2\}_k \qquad (1)$$

where $S_o(f)_k$ is the peak target power and $E\{\mathbf{Y}^2\}_k$ is the average interference-plus-noise power at the output of the kth filter [2]. The largest of the k output signal-to-interference ratios is taken to represent the output signal-to-interference ratio for the filter bank, $(SIR)_o$. Probability of detection at the filter bank output (P_d) is calculated using an empirical formula by Albersheim [3]. Probability of false alarm (P_{fa}) is assumed constant at 10^{-6}. Results are presented graphically for easy comparison.

B. Optimum Filters

The optimum (or matched) filter is used as a performance benchmark for both the eight- and five-pulse waveforms. This provides a filter set that maximizes the signal-to-clutter-plus-noise ratio for a given clutter scenario and a set of hypothesized target Dopplers [4]. The matched filter weight vector $\mathbf{w}_{opt}$ at Doppler frequency f is defined for both cases by:

$$\mathbf{w}_{opt}(\mathbf{f}) = \mathbf{K}^{-1}\mathbf{s}(\mathbf{f}) \qquad (2)$$

where, for n pulses, s represents the known target signal vector at Doppler f, and **K** the n-by-n total interference covariance matrix for the clutter scenario under investigation [5]. Here the target is assumed to be a high fixed amplitude, constant velocity, point target that can appear anywhere in the unambiguous Doppler interval. For a given clutter model, output signal-to-interference ratio and probability of detection are calculated for the eight- and five-pulse optimum filter weights. The optimum filter weights are also used as the means for generating new sets of adaptive filters for each clutter scenario (see 'Adaptive Coefficient Filters' below).

C. Clutter Modeling

In order to define the total interference covariance matrix **K**, the power spectral density for each type of interference to be included in the analysis must be known. Three types of interference are used: zero-mean Gaussian ground clutter, zero dB white Gaussian system noise, and rain clutter. The ground clutter and system noise are analytically derived and remain static throughout the analysis; only the rain clutter is allowed to vary from scenario to scenario. Four rain clutter scenarios are used, with power spectra generated from real I&Q radar data that were collected via the ASR-9's Weather Systems Processor (WSP) [6]. The WSP base data image from which these power spectra were derived is shown in Fig. 1. These are low- to medium-intensity stratiform rain storms with varying levels of reflectivity, mean velocity, and standard deviation. The power spectra for all four clutter scenarios are shown in Fig. 2. Rain Example One has frequency content that is fairly narrow but very close to the first blind speed of the radar. Rain Example Two shows a storm cell with greater frequency spread and more nonzero Doppler velocity content. Rain Example Three is a low-reflectivity case near the center of the Doppler interval. Finally, Rain Example Four illustrates how frequency-diverse a rain cell can be, with over half of the unambiguous Doppler affected by rain clutter.

D. Fixed Coefficient Filters

The fixed filter coefficients employed in the production ASR radars are not used in this analysis. However, fixed coefficient filters are generated for the analysis that are representative of the Doppler filters currently utilized by the modern ASR radars. Filter banks are generated for both the eight- and five-pulse waveforms. For the eight-pulse case, the filter bank consists of two zero-velocity filters and six nonzero-velocity filters. The five-pulse filter bank contains one zero-velocity filter and four nonzero-velocity filters. Magnitude plots for the eight-filter bank and the five-filter bank are given in Fig. 3 and Fig. 4, respectively.

E. Adaptive Coefficient Filters

For each rain scenario, new eight- and five-filter banks of

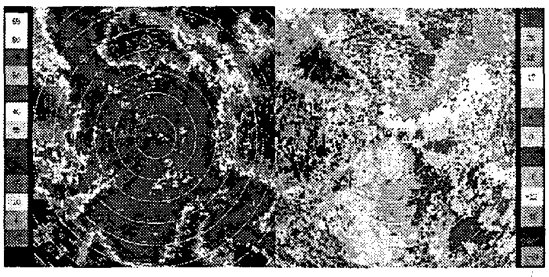

Fig. 1: Weather Base Data Image from Austin, Texas WSP Data File (left--reflectivity, right--mean velocity)

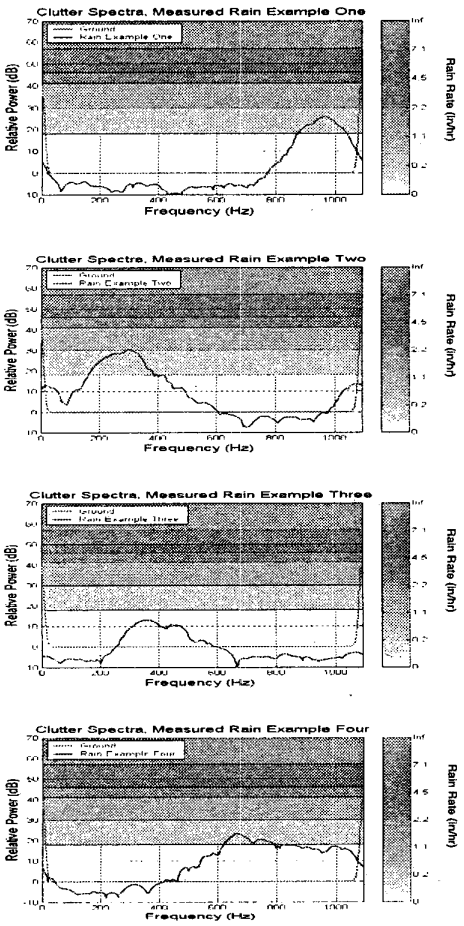

Fig. 2: Clutter Power Spectra, Measured Rain Examples 1 - 4 (measured rain spectra plus analytically derived ground clutter, noise floor at 0 dB)

nonzero-velocity Doppler filters are selected at specified Dopplers from the eight- and five-pulse optimum filter weight matrices. The zero-velocity filters remain as defined for the fixed coefficient filter banks (peaks at ±10% of the pulse repetition frequency for the eight-pulse case, and at zero Doppler for the five-pulse case). An initial set of adaptive nonzero-velocity filters is selected such that the filter peaks are equally spaced over the unambiguous Doppler interval between the zero-velocity filter peaks. For the eight-pulse case, this yields initial nonzero-velocity filters centered at 234, 358, 482, 606, 730, and 854 Hz. For the five-pulse case, the initial nonzero-velocity filters are at 218, 436, 654, and 872 Hz. For performance comparison, additional nonzero-velocity filter sets are selected from the optimum weights with center frequencies that are offset from the initial sets by deltas of ± 25 Hz, ± 50 Hz, ± 75 Hz, and ± 100 Hz, yielding a total of nine adaptive Doppler filter sets for each waveform. The output signal-to-interference ratio is calculated for every filter set. That filter set which demonstrates the lowest mean-squared-error between its output signal-to-interference ratio and that for the appropriate

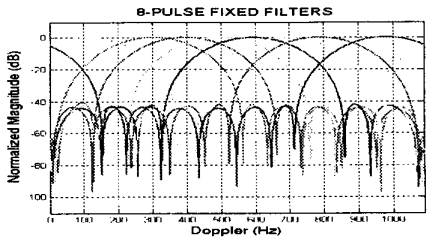

Fig. 3: Magnitude Plots, 8-Pulse Fixed Coefficient Filters

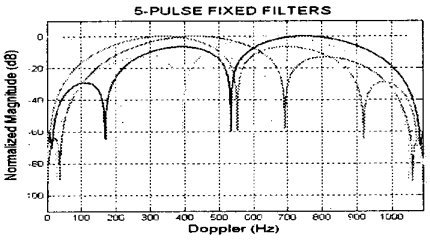

Fig. 4: Magnitude Plots, 5-Pulse Fixed Coefficient Filters

optimum is selected as the new adaptive filter set for that rain scenario. As an example, magnitude plots for the eight- and five-pulse adaptive filter sets for measured rain example 2 are shown in Fig. 5 and Fig. 6, respectively.

III. Results

A. Benefits of Integrating More Pulses

Fig. 7 and Fig. 8 show the eight- versus five-pulse probability of detection and output signal-to-interference curves

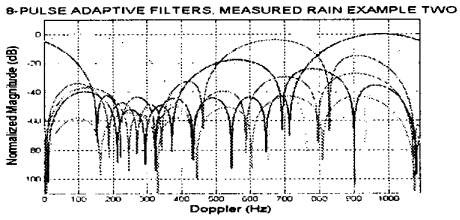

Fig. 5: 8-Pulse Adaptive Coefficient Filters, Measured Rain Example 2

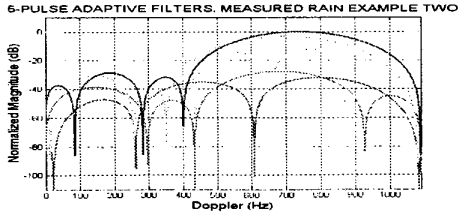

Fig. 6: 5-Pulse Adaptive Coefficient Filters, Measured Rain Example 2

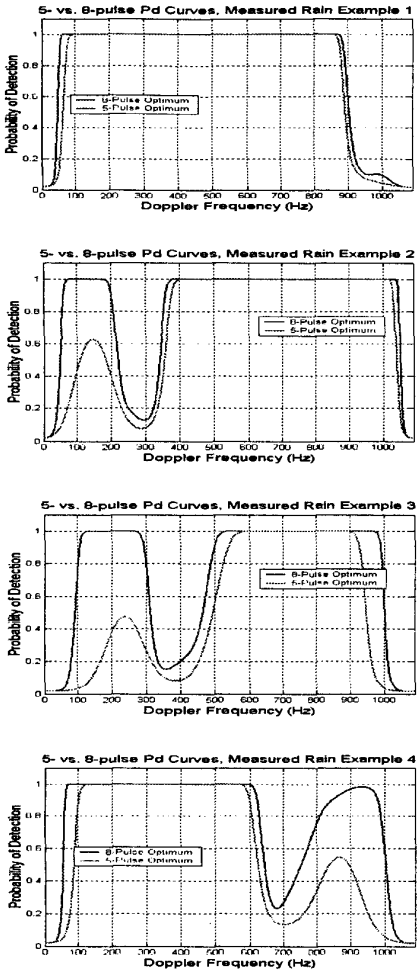

Fig. 7: 8- vs. 5-Pulse Optimum Probability of Detection Curves, Measured Rain Examples 1 - 4

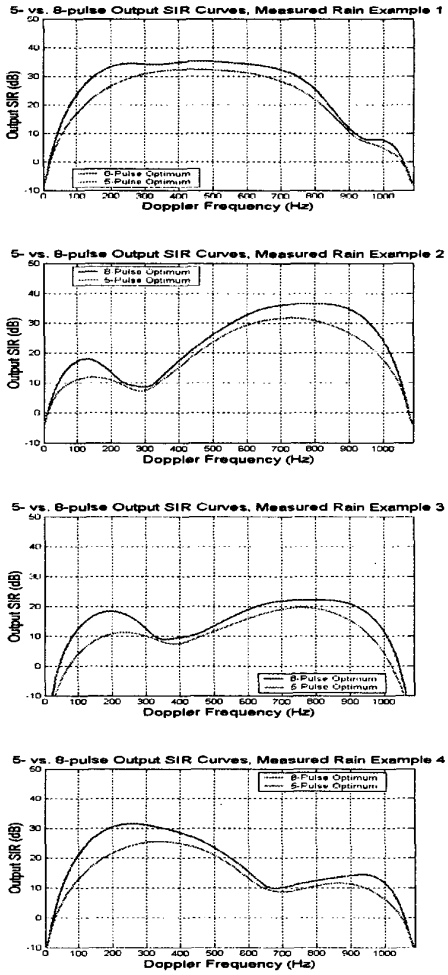

Fig. 8: 8- vs. 5-Pulse Optimum Output SIR Curves, Measured Rain Examples 1 - 4

(respectively) for the optimum filter weights, given the four clutter scenarios. Examining Rain Example One, similar detection performance is noted for both waveforms over the entire Doppler interval. In the clutter-free frequencies (100 - 800 Hz) both waveforms exhibit excellent detection; note that the detection probability does not vary in this region in either case due to the high signal-to-interference ratio. But, in the vicinity of the first blind speed where both rain and ground clutter are present, there is little detection capability with either waveform. Because the rain and ground clutter are closely spaced in frequency, the eight-pulse waveform can offer no performance advantage over the five-pulse waveform despite its higher Doppler resolution. Turning to Rain Examples Two and Three, however, it is clear that, when the rain clutter is suitably offset in frequency from the ground clutter, the higher Doppler resolution and increased coherent integration gain of the eight-pulse waveform results in better detection in the vicinity of the rain when compared to that of the five-pulse waveform. In Rain Example Four, where the rain clutter is distributed over more than half of the Doppler interval and Doppler resolution becomes less of an advantage, the eight-pulse waveform still offers better detection over the five-pulse waveform due to its higher coherent integration gain.

B. Fixed vs. Adaptive Coefficient Filters, 8-Pulse Waveform

Fig. 9 illustrates the probability of detection and output SIR results when using the eight-pulse adaptive coefficient filters versus the eight-pulse fixed coefficient filters for rain clutter scenario 2. The eight-pulse optimum probability of detection and SIR curves are shown for reference. Though only one example is shown here, in all cases where the rain has nonzero Doppler velocity (Examples 2 - 4), the adaptive coefficient filters offer significantly better probability of detection,

particularly in the vicinity of the rain clutter. Both filter sets perform well when the weather is near the first blind speed (Example 1). Table 1 lists the probability of detection percentages (calculated as area under the probability of detection curves) for each filter set (optimum, fixed, and adaptive) and each rain scenario.

C. Fixed vs. Adaptive Coefficient Filters, 5-Pulse Waveform

Fig. 10 illustrates the probability of detection and output SIR results when using the five-pulse adaptive coefficient filters versus the five-pulse fixed coefficient filters for rain clutter scenario 2. The five-pulse optimum probability of detection and SIR curves are shown for reference. Again, though only one example is shown, in all cases where the rain has nonzero Doppler velocity (Examples 2 - 4), the adaptive coefficient filters offer significantly better probability of detection, not only in the vicinity of the rain clutter but across the entire unambiguous Doppler interval. As before, both filter sets perform well when the weather is near the first blind speed (Example 1). Table 2 lists the probability of detection percentages (calculated as area under the probability of detection curves) for each filter set (optimum, fixed, and adaptive) and each rain scenario.

D. Performance with Low Amplitude Target Parameters

In all of the above examples, the target amplitude was chosen at an arbitrary, high, constant level relative to the peak weather amplitude to better illustrate the effects of integrating more pulses and using the adaptive Doppler filtering technique. It can be seen by examining the output SIR curves that, because of the high target amplitudes, the analysis is being done in an optimistic region of the probability of detection curves. While this analysis is reasonable, it is beneficial to demonstrate what happens when the target amplitude is reduced to a more representative level.

Assume that, for both systems, the range equation yields a 3 dB single-pulse signal-to-noise ratio for a 1-m^2 target at 55 nautical miles. Placing this target at 25 nautical miles generates a 16.7 dB input signal-to-noise. The analysis using rain clutter example 2 for both the eight- and five-pulse fixed and adaptive filters is repeated with this target, and the results are shown in Fig. 11 and Fig. 12, respectively.

There are several points to note with these results. First, while optimum detection in both the eight- and five-pulse cases is somewhat diminished versus the previous examples, the eight-pulse case achieves reasonable detection in those areas not impacted by the rain clutter (600 - 900 Hz). The five-pulse optimum detection is less than 80% across the entire Doppler interval. Also, the eight-pulse fixed filters show a clear advantage in this rain scenario, achieving nearly optimum detection while the five-pulse filters have nearly zero detection. These results are due to a combination of the better filter

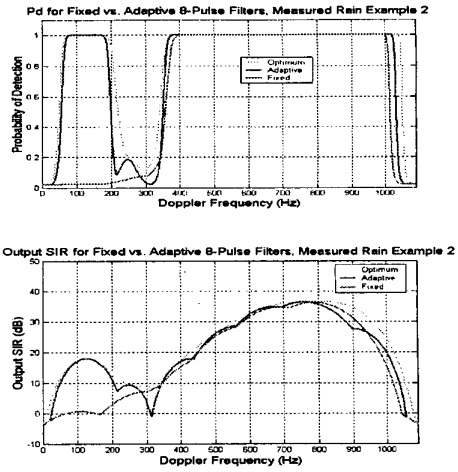

Fig. 9: Pd and Output SIR Results for Fixed vs. Adaptive 8-Pulse Filters, Measured Rain Example 2

TABLE 1
PROBABILITY OF DETECTION FOR 8-PULSE FIXED VS. ADAPTIVE COEFFICIENT FILTERS, RAIN EXAMPLES 1 - 4

	Rain Example 1	Rain Example 2	Rain Example 3	Rain Example 4
8-Pulse Optimum Filters	80.0%	82.3%	71.8%	77.3%
8-Pulse Fixed Filters	75.1%	61.8%	45.1%	52.9%
8-Pulse Adaptive Filters	76.6%	77.1%	65.4%	68.6%

resolution and coherent integration gain seen with eight pulses as opposed to five. As noted before in the previous examples, the adaptive filtering technique generates near-optimum results in both the eight- and five-pulse cases.

IV. CONCLUSIONS

The coherent integration of more pulses provides the expected detection benefits against distributed clutter. A significant advantage in terms of Doppler resolution is also noted when integrating eight pulses as opposed to five, resulting in higher detection probabilities in the vicinity of nonzero-Doppler rain clutter when it is suitably offset from zero Doppler. In cases where increased detection performance is desired but waveform alterations to increase the number of pulses integrated are not viable, an adaptive filtering approach may provide substantial detection improvement against moving clutter versus that seen

with fixed coefficient filtering techniques. Further study would be required to investigate real-time implementation and the feasibility of applying this technique to production systems.

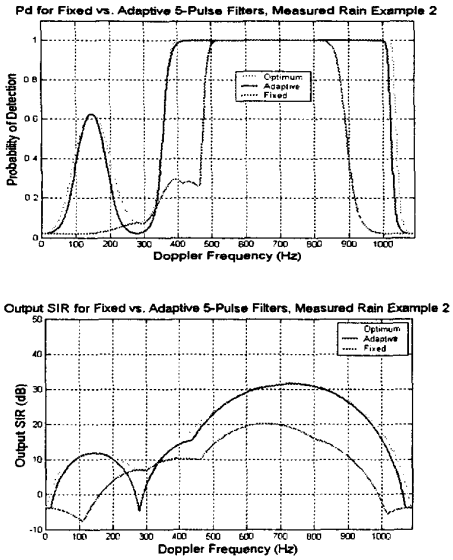

Fig. 10: Pd and Output SIR Results for Fixed vs. Adaptive 5-Pulse Filters, Measured Rain Example 2

TABLE 2
PROBABILITY OF DETECTION FOR 5-PULSE FIXED VS. ADAPTIVE COEFFICIENT FILTERS, RAIN EXAMPLES 1 - 4

	Rain Example 1	Rain Example 2	Rain Example 3	Rain Example 4
5-Pulse Optimum Filters	77.1%	71.2%	49.1%	59.1%
5-Pulse Fixed Filters	74.3%	43.4%	32.3%	39.1%
5-Pulse Adaptive Filters	75.7%	67.9%	46.8%	55.7%

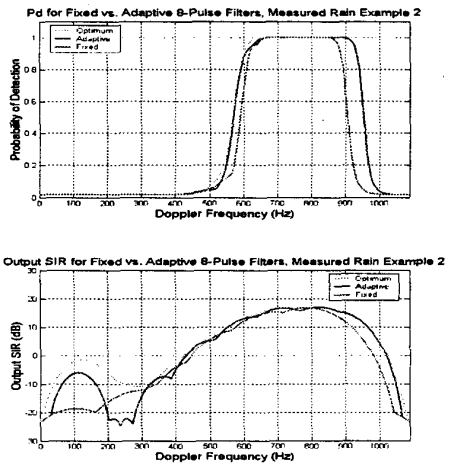

Fig. 11: Pd and Output SIR Results for Fixed vs. Adaptive 8-Pulse Filters, Measured Rain Example 2 (1-m^2 target at 25 nautical miles)

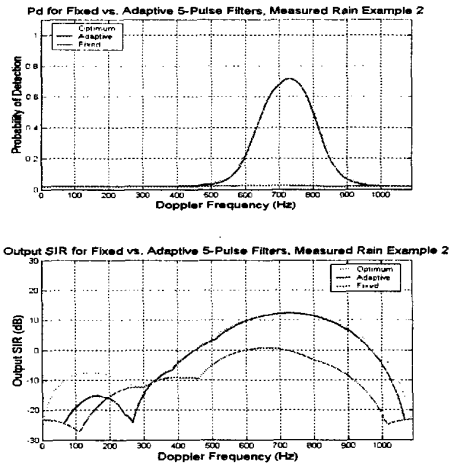

Fig. 12: Pd and Output SIR Results for Fixed vs. Adaptive 5-Pulse Filters, Measured Rain Example 2 (1-m^2 target at 25 nautical miles)

REFERENCES

[1] Meuhe, C. E., "Digital Signal Processor for Air Traffic Control Radars". NEREM 74, Part 4: Radar Systems and Components, pp. 73-82, October 1974.

[2] Stark, Henry and Woods, John W. *Probability and Random Processes with Applications to Signal Processing*, 3rd edition. New Jersey: Prentice-Hall, 2002.

[3] Skolnik, Merrill I. *Introduction to Radar Systems*, 3rd edition. New York: McGraw-Hill, 2001.

[4] DeLong, D.F., and Hofstetter, E. M., "On the Design of Optimum Radar Waveforms for Clutter Rejection". IEEE Transactions on Information Theory, Volume IT-13 No. 3, pp. 454-463, July 1967.

[5] Ludloff, A.. et al, AEG-Telefunken, "Doppler Processing Waveform Design and Performance Measures for some Doppler and MTD Radars". Reprint from 'Ortung and Navigation', March 1981 (pp. 417-456) and January 1982 (pp. 5-54).

[6] Weber, M. E., "ASR-9 Weather Systems Processor (WSP) Signal Processing Algorithms". MIT Lincoln Laboratory Project Report ATC-255, June 2002.

[7] Haykin, Simon *Adaptive Filter Theory*, 4th edition. New Jersey: Prentice-Hall, 2002.

[8] Kay, Steven M. *Modern Spectral Estimation Theory & Application.* New Jersey: Prentice-Hall, 1988.

[9] McDonough, Robert N. and Whalen, Anthony D. *Detection of Signals in Noise*, 2nd edition. San Diego: Academic Press, 1995.

[10] Oppenheim, Alan V. and Schafer, Ronald W. *Discrete-Time Signal Processing* , 2nd edition. New Jersey: Prentice Hall, 1999.